# Synchronization and Control Strategies for Vehicle-to-Grid Operation to Utilize Electric Vehicle Batteries for Supporting Power Grid

NHAT NGUYEN, CHRIS CHU, HA THU LE*
Department of Electrical and Computer Engineering
California State Polytechnic University, Pomona, USA
3801 West Temple Avenue, Pomona, California 91768
UNITED STATES OF AMERICA

*Corresponding Author*

*Abstract*: - Recent advancements in battery technology have made electric vehicles (EV) more affordable, leading to their increased use around the world. However, the increase in EV numbers is creating pressure on the power system, where the high power demand for EV charging is causing grid overload in multiple areas, resulting in voltage instability. This study investigates the use of EV chargers and batteries for vehicle-to-grid (V2G) applications. We used Synchronous Reference Frame Phase Lock Loop (SRF-PLL) technique and phase compensation to design a synchronization system for EV chargers in V2G operation. An internal 60-Hz power source is incorporated in the SRF-PLL system to enable EV chargers to operate in inverter mode during grid outages. In addition, a control strategy is considered for exploiting EV battery packs to stabilize grid voltage. Key research outcomes include effective synchronization of EV charger with grid, improved voltage stability, faster system response, and enabled usage of EV battery packs for multiple consumer applications. The outcomes help extend EV capability, broadening their practical use for both the vehicle owners and power grid operators. This, in turn, contributes to accelerating adoption of EVs for reducing harmful emissions and protecting the environment.

*Key-Words:* - Battery, bidirectional chargers, electric vehicle, power grid, phase-lock loop, vehicle-to-grid (V2G).

Received: March 4, 2026. Revised: May 2, 2026. Accepted: June 5, 2026. Published: July 9, 2026.

## 1 Introduction

The recent global oil crisis has driven up gas prices, rendering it more expensive to operate internal combustion engine (ICE) vehicles. This, coupled with stricter emission requirements worldwide to combat air pollution, has compelled major car manufacturers to shift from traditional ICE vehicles to more environmentally friendly and energy-efficient electric vehicles (EV). Many governments have initiated various policies and programs to promote the adoption of clean vehicles. For instance, the US provides buyers up to $7500 in tax credits for purchasing eligible clean vehicles, [1]. The surge in EV numbers in the upcoming years is easily foreseeable. Infrastructure for the increasing power demand plays a pivotal role in advancing EV adoption, [2]. Improvements in power transmission and distribution must be addressed to ensure the delivery of reliable power.

Electric vehicles are challenging loads for many power distribution networks. A typical U.S. single-family house has a peak demand of 5 kW. Tesla S, for example, has a battery capacity of 100kWh and a range of up to 405 miles. At Level 2 charging of 240V, it takes about 8 hours to fully charge the car and the power drawn during that time is around 12.5 kW. It follows that the Tesla S power demand is higher than the peak demand of a single-family house by 2.5 times. Its charging can create overloading of the host distribution feeder. The problem is intensified when millions of EV penetrate the distribution networks. The problem is worsened by the fact that EVs move and can charge anywhere. This poses another big challenge for power system operators to predict the demand and schedule supply (generation). Furthermore, dynamic distribution of EV can overload some parts of the power networks while leaving other parts under-loaded. Both overloading and underloading conditions increase power system operation cost, lower equipment efficiency, and create power quality problems, such as voltage sag and voltage swell. On the positive side, EV battery power may be discharged to support power system operation during daily peak hours, loss of supply capacity (e.g. loss of a big generator), and other emergency conditions, [3], [4], [5], [6], [7], [8], [9], [10], [11].

EV charging demand is anticipated to be increasing in many residential areas. The elevated power demand during peak hours may result in frequency fluctuations, sudden voltage drops, and strain on power transmission equipment. Utilities may need to employ additional power generators to meet the EV demand, leading to higher operation cost.

Vehicle-to-Grid (V2G) is envisioned to be a promising technology for solving the EV charging pressure on the grid. Using V2G, EV battery DC power is converted to AC using an inverter and channeled into the grid at times of need to support its operation. To maintain the grid stability and power quality, the AC signal from the grid-tied inverter must be synchronized with the grid where the inverter output voltage phase angle and frequency must be the same, or remarkably close, to those of the grid connection point. This research investigates a method called synchronous rotating frame phase lock loop (SRF-PLL) for synchronizing the output signal of EV chargers with the grid when operating in inverter mode. Synchronization of the EV charger output with the grid is a core requirement for enabling their V2G operation. Further, some EV battery control strategies are also considered for maintaining grid voltage stability. MATLAB Simulink is used for simulation and analysis.

### 1.1 Integration of EV Into the Existing Energy Eco System: Power Demand, Grid Stress and Instability, Utilization of EV Battery Packs

The increasing number of electric vehicles raises the power demand on the electrical grid significantly, especially during their peak charging periods. Such a demand surge puts considerable stress on the outdated electrical infrastructure. Consequently, the electrical grid must be extensively upgraded to accommodate the higher loads due to the widespread EV adoption, [12].

Geological characteristics of charging stations and residential areas also play an important role in contribution to the grid demand. Charging stations are often strategically located, concentrated in specific geographic regions where EV adoption is high. Such areas experience a more profound surge in power demand due to clustering of load. The demand surge negatively affects the residential and business establishments near these stations, as well as the local distribution feeders that supply the stations.

With the foreseen popularity of EVs in the near future, localized spikes in power demand create many challenges for grid management to counter the negative effects of mass EV charging. The simultaneous charging of numerous EVs introduces fluctuations that disrupt grid stability. Sudden voltage drops and frequency variations also challenge the reliability of the power system, [12], [13]. These negative effects include damage to electronics and reduced lifespan on electric appliances. Grid-scale power surges can cause immediate damage to electronic components in delicate appliances. Sensitive electronics parts such as microprocessors and circuit boards may also suffer irreversible damages. Frequent electric spikes exposure can reduce the lifespan of appliances significantly. This leads to the wear and tear of internal components, negatively affecting the overall durability of the appliances, [12], [13].

Businesses with electronic storage, such as computers, cloud servers, or smart devices may also suffer from grid instability. Data loss is caused by sudden power surges that can negatively affect the business, resulting in loss of revenue, infrastructure damage, and decrease overall effectiveness of electrical equipment. In some cases, power surges can even pose fire hazards, due to the overheating of internal components with increased voltage during power spikes, [13].


Fig. 1: Tesla charging stations. The station with plugged-in EVs can be exploited as a clustered energy storage to support the power grid
*Source: [14].*

Concentrated charging may also lead to the imbalance of load, [12]. Those areas near commercial charging stations may experience heightened demand while others remain underutilized, making distribution and resource balancing become more challenging. Navigating the distinct characteristics of uneven load distribution has become a main challenge for utilities to ensure power quality and stability of the electrical grid.

The increasing number of electric vehicles with their battery packs offer significant energy potential to contribute to grid stability through a method known as Vehicle-to-Grid (V2G). The surplus energy stored in EV batteries can be effectively harnessed to improve grid stability, particularly during peak demand periods or emergency scenarios. Bidirectional charging technology enables EVs to function as mobile energy storage systems, migrating the conventional role of energy consumers to dynamic contributors to the electrical power grid.

During instances of increased demand, when the grid faces strain and requires additional power, battery packs can discharge stored energy to relieve strain on the grid and act as decentralized energy resources that respond dynamically to grid conditions. A charging station like that of Figure 1 with EVs being plugged-in can be exploited as a clustered energy storage for supporting the grid. Figure 2 demonstrates multiple vehicles with V2G technology. With the ability to relocate, V2G technology also implements load balancing by redistributing electricity from vehicles with excess energy to regions facing shortages, optimizing resource allocation across the grid, and averting overloads or blackouts during peak consumption.

Conversely, during periods of low demand, EVs can absorb excess power, serving as a buffer to absorb surplus energy and prevent grid instability. The load balancing ability of EVs ensures power is distributed efficiently, thus optimizing energy consumption and minimizing the likelihood of power surges caused by uneven distribution.

## 1.2 Energy Cost Saving Potential

The incorporation of V2G technology marks a notable shift in the energy landscape, particularly concerning the economic benefits for electric vehicle owners. For example, Figure 3 and Figure 4 show different pricing models of Southern California Edison, a large electric utility in California, according to various months of the year. During off-peak hours, EV owners can charge their batteries at a low price. Later, during peak hours, when electricity demand and price are high, EV owners can benefit from selling the battery energy at premium rates.

This mutual interaction between the EVs and the grid brings practical advantages for EV owners, especially in terms of economic benefits, [12]. It transforms EVs into assets that can generate income to offset the initial investment and charging costs. The buy-low sell-high scheme only reduces the overall cost of owning an EV but also positions the owners as contributors to grid stability.

The Vehicle-to-Grid scheme can potentially bring lots of benefits to EV owners who can make considerable additional income by charging during off-peak hours and sell (i.e., discharge) power back to the power system during peak hours. A utility price for electricity during off-peak hours is around 25 cents per kWh and 49 cents per kWh during peak hours (4pm-9pm), [15]. The profit that can be made is up to 24 cents per kWh. A Tesla S, [11], owner can sell 70% of its battery capacity (70kWh) to grid per day, leaving 30 kWh (120 miles) for the owner's travel need. This way, the owner can make up to $500 per month, or up to $6,000 per year. The trading scheme requires up to one additional charge-discharge cycle per day, or up to 365 cycles per year. This will lower the battery life span to some extent but the extra income of up to $6,000 per year can outweigh the life span impact.

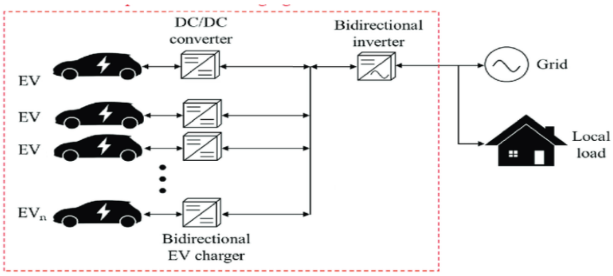

Fig. 2: Multiple EV battery energy storage
*Source: [16].*

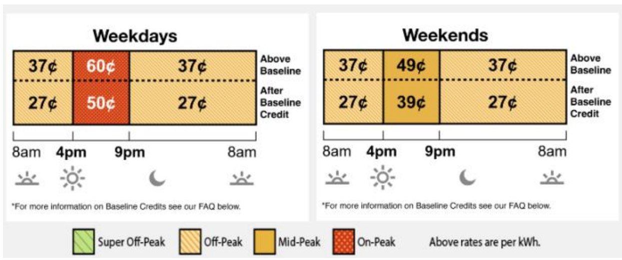

Fig. 3: SCE Time-of-Use (TOU) June-September
*Source: [15].*

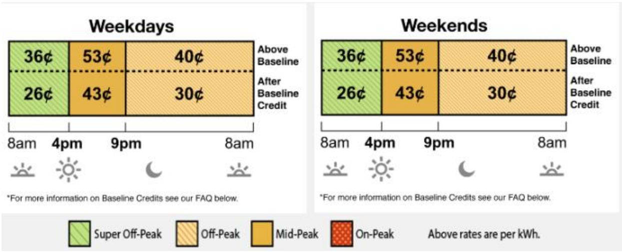


Fig. 4: SCE Time-of-Use (TOU) October-May
*Source: [15].*


Fig. 5: Bidirectional charging eco system
*Source:[17].*

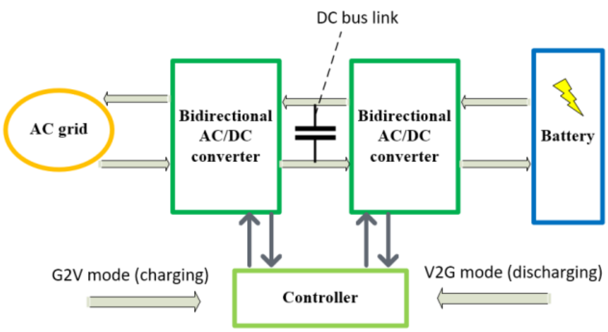


Fig. 6: EV bidirectional charger topology
*Source: [18].*

## 1.3 EV and Renewable Energy

Combining bidirectional charger technology with renewable energy aligns with the goal of building a sustainable and resilient energy infrastructure, [12]. Using EVs as energy storage units addresses the intermittency of solar and wind power, improving grid stability and ensuring a more dependable energy supply. Figure 5 demonstrates the eco system of what would be built in the future to incorporate bidirectional charging technologies with renewables.

The integration of bidirectional charger technology with renewable energy sources, such as solar and wind power, represents a key step in fortifying the reliability of the power system. Bidirectional chargers allow EVs to not only consume energy but also store surplus power generated from renewables. This is especially helpful when renewable sources produce excess energy. Such energy can be directed to charging EV batteries, creating a flexible energy storage system.

Moreover, the nature of renewable energy sources, such as solar and wind power, is characterized by fluctuations in energy production, influenced by weather conditions and time of day. EV batteries act as efficient storage units, allowing the capture and retention of excess energy during peak production periods. One main benefit of integrating bidirectional charging technology with renewables is the ability to smooth out the variability in energy generation.

During the time of low demand when solar panels and wind turbines generate surplus electricity, rather than letting it go to waste, the energy can be stored in EV batteries without the need to invest in an additional energy storage system. This stored energy can then be tapped into during periods of reduced energy production, ensuring that power supply is consistent and reliable.

Furthermore, stored energy in EV batteries provides a buffer against sudden drops in renewable energy output due to uncontrollable factors such as cloud cover or calm wind. This buffer helps mitigate the impact of intermittent energy generation, contributing to grid stability and reducing the reliance on supplementary power sources during fluctuations.

## 1.4 Bidirectional Charger and Control

A bidirectional charger is a device that connects an electric vehicle and an external source and enables the flow of electricity in two directions between them, [19]. Unlike traditional chargers, which only allow the current flow from the power supply to the EV battery, a bidirectional charger can be used in both charging and discharging scenarios, [2]. Figure 6 shows the topology of a bidirectional charger. These chargers enable power flow in two directions, allowing the EV battery to act as a mobile energy storage system that can supply electricity to the grid during peak demand periods or in emergency situations. Figure 7 and Figure 8 show some bidirectional charging systems where the latter has V2G capability.

However, integration of a bidirectional charger without a robust control method introduces several disadvantages that defeat its effectiveness of operation within the energy ecosystem, particularly in the context of power spikes and grid fluctuations during peak hours. With the absence of a control mechanism, the bidirectional charger struggles to synchronize with the grid frequencies, causing potential issues such as frequency variations and voltage instability.

During peak hours operation, when the power demand for electricity is highest, sudden power spikes can occur, causing significant challenges for the EV charger system without a robust control method integrated. Failing to adapt to rapid changes in the grid conditions leading to disruptions in grid power quality. In order to curb these challenges and ensure grid stability, the authors of this article propose a robust closed-loop control system. It employs a feedback mechanism to continuously monitor and adjust charger operation based on the grid conditions. By actively regulating power flow and responding to grid dynamics in real-time, synchronizing frequencies and voltage levels between the charger and the grid, the robust control system help minimize phase differences and maintain grid power quality.

### 1.5 Grid-tied Inverter Concepts

Grid connected inverters are electronic devices used in bidirectional chargers and renewable energy systems as interfaces with the power grid. They convert the battery DC power or the power generated by the renewable sources to AC power of required frequency that can be fed into the grid. Figure 9 shows the basic components of a simple grid-tied inverter.

Grid-tied inverters must comply with power quality standards to ensure the stability of the grid. This includes a proper voltage and frequency that matches the voltage and frequency of the grid. However, the grid conditions frequently change due to diverse factors, such as load variation, generation changes, and other disturbances. These changes can cause a phase shift between the inverter output and the grid voltage. Significant change in phase of the grid can have a negative effect on the power quality and the stability of the grid-tied inverters. Therefore, the authors focus on developing a synchronization system for grid-tied inverters in EV bidirectional chargers.

## 2 Phase Locked Loop (PLL) and MATLAB Simulink Implementation

### 2.1 Different Types of PLL

A PLL is considered for the synchronization system of EV bidirectional chargers. There are many types of PLL available but mainly divided into open-loop and closed-loop PLL. Open-loop control such as zero- crossing method is a simple way to figure out how often a signal goes through zero and to get information about its phase. In devices like converters that change AC to DC using triacs or thyristors, the zero-crossing method helps determine when to start the pulses that control the process, [20].


Fig. 7: Ford Charge Station Pro
*Source: [21].*


Fig. 8: Fermata Energy FE-20
*Source: [22].*

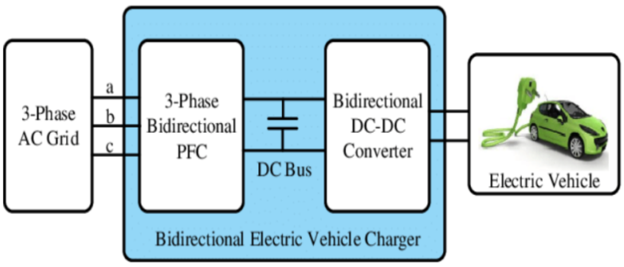


Fig. 9: Three-phase grid-tied inverter
*Source: [23]*

While the zero-crossing method boasts simplicity and minimal computational demands, it comes with significant drawbacks. The updating rate is slow as frequency information is available only every half cycle. Additionally, its assumption of constant frequency in at least one-half cycle may not always hold, making it prone to phase jumps during the activation or deactivation of large loads and variations in the grid frequency. The presence of harmonic components can lead to multiple zero-crossings, distorting the input signal. Accuracy in detection may further be compromised by biases in the analog-to-digital converter (ADC) or the comparator circuit, emphasizing the need for precise system calibration, [20].

Another method is called Second Order Generalized Integrator Phase-Locked Loop, or SOGI-PLL. It is a sophisticated control technique employed in grid-tied inverters to synchronize their output voltage with the grid. Unlike traditional PLLs, SOGI-PLL offers advantages such as enhanced accuracy, faster response to dynamic changes in the grid frequency, and robust performance in the presence of grid disturbances, [24]. This method employs second-order integrators to provide both frequency and phase information, allowing for a precise and rapid response to variations in the grid, [24]. While SOGI-PLL addresses some of the limitations of conventional PLLs, such as slow updating rates and vulnerability to phase jumps, it may have increased computational requirements and it is known to be sensitive to DC offset and low-order harmonics in the input signal, which may lead to accuracy issues and affect its performance, [24].

This study selects a method called synchronous rotating frame phase lock loop (SRF-PLL) for developing the synchronization system for EV bidirectional chargers.

The trade-off between complexity and performance guides the selection of the SRF-PLL, which excels in situations demanding high precision, robustness, and adaptability in dynamic grid conditions. The following section discusses fundamental concepts of SRF-PLL.

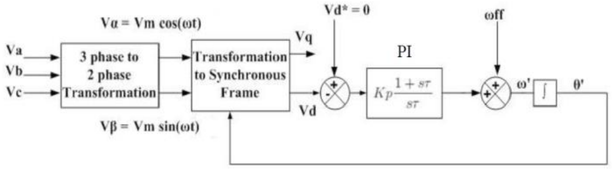


Fig. 10: SRF-PLL feedback mechanism
*Source: [25]*

## 2.2 Synchronous Rotating Frame PLL Fundamentals

The fundamental operation of the SRF-PLL is using a feedback mechanism together with a PI-regulator to detect and track the phase angle of the input signals, as shown in Figure 10. The input signal of the PLL is taken from the three phases of the utility grid voltage and the generated output of the feedback control loop is the phase angle of one of these phases.

The SRF-PLL is commonly used in communication systems to synchronize the transmitted and the signal received. It also has extensive applications in motor control, radar systems, GPS receivers, frequency synthesis and audio processing, [25]. As mentioned previously, we use the SRF-PLL for Vehicle-to-Grid application, where precise synchronization between the grid and the output signal of the EV grid-tied inverter is required to comply with the grid voltage and frequency synchronization requirements, as well as to maintain grid power quality.

### 2.2.1 Stationary Reference αβ Frame, [25]

Referring to the SRF-PLL diagram in Figure 10, the input voltage from the grid can be written as

$$\begin{bmatrix} V_a \\ V_b \\ V_c \end{bmatrix} = \begin{bmatrix} V_m \sin(\theta) \\ V_m \sin(\theta - \frac{2\pi}{3}) \\ V_m \sin(\theta + \frac{2\pi}{3}) \end{bmatrix} \tag{1}$$

where $V_m$ is the maximum value of the voltage. The angle $\theta$ $(2\pi f t)$ changes with time and represents the phase of $V_a$ voltage since the voltages signal are function of time and frequency, [25]. In natural frame, the three-phase coordinates are evenly distributed by $\frac{2\pi}{3}$ rad from each other. To implement the phase angle detection of grid voltage signals, $V_{abc}$ are fed through a 3-phase to 2-phase transformation block to generating the two-phase stationary reference system $V_\alpha$ and $V_\beta$.

The transformation of natural frame to stationary reference frame is called Clarke transform or $abc \to \alpha\beta$ transformation. The Clarke transform is written as:

$$\begin{bmatrix} v_\alpha \\ v_\beta \end{bmatrix} = T_{\alpha\beta} \begin{bmatrix} v_a \\ v_b \\ v_c \end{bmatrix} \tag{2}$$

$$T_{\alpha\beta} = \frac{2}{3}\begin{bmatrix} 1 & -\frac{1}{2} & -\frac{1}{2} \\ 0 & -\frac{\sqrt{3}}{2} & \frac{\sqrt{3}}{2} \end{bmatrix} \quad (3)$$

Performing calculation for $V_{\alpha\beta} = T_{\alpha\beta} \times V_{abc}$, we get:

$$\begin{bmatrix} V_\alpha \\ V_\beta \end{bmatrix} = \begin{bmatrix} V_m \sin(\theta) \\ V_m \cos(\theta) \end{bmatrix} \quad (4)$$

### 2.2.2 Synchronous Rotating Reference Frame dq0 Transformations, [25]

After transforming the grid reference 3-phase voltage, $V_a, V_b, V_c,$ into 2-phase, $V_{\alpha\beta}$, the obtained alpha-beta signal is channeled through dq0 block (the 2nd box from left in Figure 10). The output is denoted $V_d, V_q$ components. To align the d-axis with $V_a$ from the grid signal, we need to make $V_q$ =0 and obtain the new angle $\omega t$. The transformation rotates the coordinates of the phase angle to align the d-axis with the instantaneous phase of the signal. This is achieved by comparing $V_q$with a constant 0 then feeding it through the PI controller to obtain the angle $\omega t$. Integrating the angle $\omega t$ will give us the theta angle, this angle be looped back to the dq0 block, completing the PLL, [25].

The reference signal represented in the $dq$ frame makes control algorithms more efficient. It also reduces the cross-coupling effects between the phase and frequency components. The control method can focus on manipulating the $d$ and $q$ components of the reference signal individually, thus, simplifying the implementation and controlling of the phase lock loop, [25].

### 2.2.3 Implementation in MATLAB Simulink

For developing the synchronization system for EV V2G application, the authors adopt the discharging system of a bidirectional charger, which was originally developed by Ha Thu Le and Chris Chu and implemented in MATLAB Simulink in [12]. The deficiency of the original discharging system is that it utilizes constant reference signals to control the switching operations of the IGBT switches. While this method is proved to keep the system functional, it does not ensure synchronization of the inverter output signal with that of the grid. Ha Thu Le and Nhat Nguyen have improved the original design as described below. The new and improved system is presented in Figure 11 (Appendix) where SRF-PLL is used for synchronization of the inverter output voltage signal with that of the power grid.

In the original design, a constant three-phase source represents the power grid. An LC filter is placed between the power source and the inverter to filter harmonics created by the IGBT switches, [12]. This design makes measuring the inverter output voltage difficult. Due to the influence of the power source, any voltage measured at this location is affected by the strong source, potentially leading to incorrect measurements.

In this study, the power source is replaced by a 240V-60-Hz load and the output of the inverter through the LC filter is measured at the load. This way, the output waveform of the inverter is not influenced by the power source. Additionally, the constant 3-phase source is replaced by a programable source, where frequency can be varied to create different phase angles, particularly, 15°, 45°, 75° and 90°. This represents various phase angles of voltages which exist at different locations on the grid. The output signal is captured to determine how long it takes the SRF-PLL to synchronize the inverter output with the reference power grid and to measure the phase difference between them.

Harmonic analysis from the original system in [12] is redone to ensure that the integration of the SRF-PLL does not introduce additional harmonics into the grid, keeping them within the acceptable range.

We also determine that the LC filter used in the original system introduces a phase shift at the output. The amount of phase shift created by the LC filter can vary and depends on the filter design parameters. For the LC filter used in this study, the phase shift is 85 degrees lagging. Therefore, we also develop a method to compensate for this 85-degree phase shift to keep the inverter output in phase with the grid reference source.

## 2 Simulation of SRF-PLL based Synchronization System for EV Charger in Discharging Operation

The proposed SRF-PLL based synchronization system works as follows. For synchronizing with the reference signal, $V_q$ needs to be zero. From the graph in Figure 12, when $V_q$ vector is zero, the $V_a$ voltage is aligned with the d-axis. To achieve this, the controller is designed to make $V_q$ components to zero. Therefore, a new angle theta is obtained through modulation of the PI controller output. The synchronous rotating frame (SRF) controls the operation of the phase lock loop. The d- and q-axis are direct and quadrature frame of the signal, respectively.

Referring to Figure 11 (Appendix) and Figure 13, the $\alpha\beta$ signal obtained from the three-phase voltage $V_a$,$V_b$ and $V_c$ of the grid reference source is fed through the dq transformation block to obtain $V_d$ and $V_q$ components. From this stage, we compare $V_q$ with zero to drive $V_q$ to zero, then feed it through a PI controller to obtain the new angle $\omega t$ (i.e., theta in radians) with $V_q$ locked to zero. The output signal obtained from the PI controller passes through an integrator. Then, the signal from the integrator, along with a constant $2\pi$, is fed to a modulo block to properly maintain the angle theta between 0 and $2\pi$. The transfer function of the PI controller can be written as:

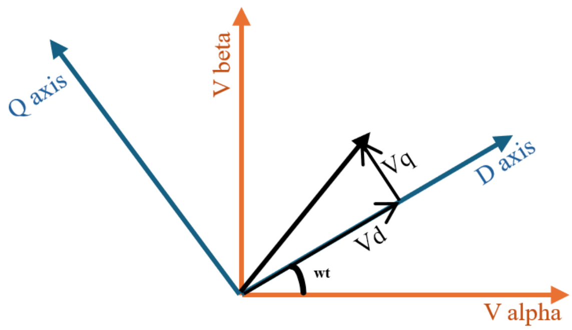


Fig. 12: Voltage components related to active/reactive axis
*Source: [25].*

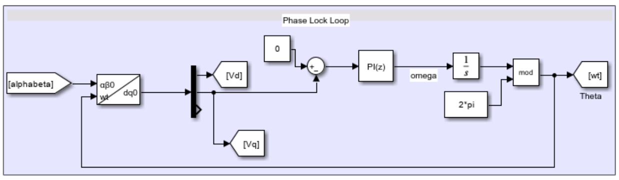


Fig. 13: Simulink phase lock loop integration.
*Source: created by the authors.*

$$G_{OpenLoop}(s) = V_m \frac{k_p s + k_i}{s} \frac{1}{s} \quad (5)$$

$$G_{ClosedLoop} s = \frac{V_m(k_p s + k_i)}{s^2 + V_m k_p s + V_m k_i} \quad (6)$$

$$w_n = \sqrt{V_m k_i} \quad (7)$$

$$\zeta = \frac{V_m k_p}{2\sqrt{V_m k_i}} \quad (8)$$

The damping ratio $\zeta$ of the PI controller is selected to be 0.7 and natural frequency of 1kHz with the grid voltage of 195.96 V, the peak value of phase $V_a$ of the grid reference signal. The new angle theta obtained after modulation block is looped back to the input of the dq transformation block, completing the phase lock loop. Since the study core objective is to synchronize the phase angle of the signal generated from the IGBT inverter with the grid, current regulation is not implemented in this work. The $V_d$ and $V_q$ components are fed through an inversed Park transformation along with the new angle theta to reconstruct a reference signal to operate the IGBT switches of the inverter. The Simulink reference signal generator for IGBT inverter is shown on Figure 14.

### 3.1 Boost Converter for Improved Discharging System

The most important part of the bidirectional charging system for EV is the discharging operation. The battery requires a DC to AC inverter to provide power to the utility grid. The output DC voltage of the battery requires to be increased or lowered accordingly to ensure the correct power required for the inverter to work properly. Initially, a buck converter was used to regulate the voltage of the battery. However, the system does not provide the correct line to line voltage after the low pass filter. After many trials, a boost converter with low duty ratio is placed between the battery and the inverter to provide the correct system output line-to-line voltage at the output of the low pass filter.

A low duty ratio boost converter can improve the system efficiency by letting the converter operate closer to the peak efficiency of the device. This effect can be enhanced when the input voltage needs to be boosted significantly. Operating at low duty ratio is also beneficial when interacting with utility grid and provides efficient power transfer. Another advantage of a low duty ratio boost converter is cost efficiency. Generally, low duty ratio converters require smaller capacitors and inductors, thus reducing the weight, cost of the device and improving mobility, which is an important factor in V2G applications. On the other hand, higher switching frequency is required to operate the boost converter at low duty ratio. In this simulation, the MOSFET is operated at 25kHz, which is within a common switching frequency range of the device. Figure 15 shows the implementation of a boost converter in MATLAB Simulink.

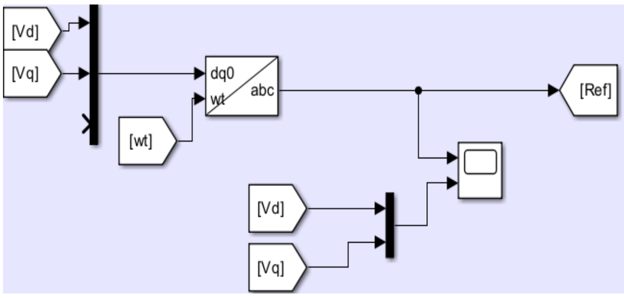


Fig. 14: Reference signal generator for IGBT inverter
*Source: created by the authors.*

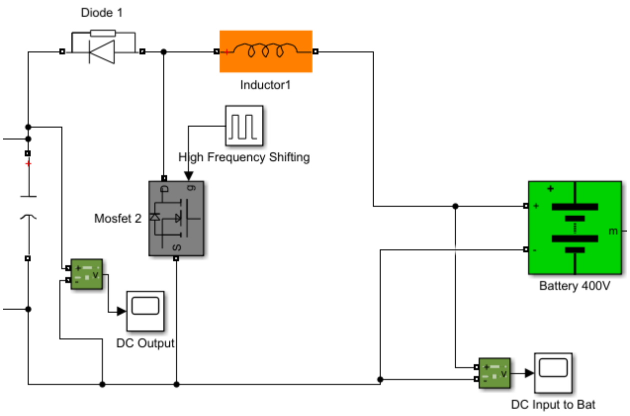


Fig. 15: Boost converter with low duty ratio between the inverter and EV battery
*Source: created by the authors.*

## 3.2 Harmonics and Filter for Improved Discharging System

Harmonics refers to the voltage or current signal with unwanted frequency deviated from the grid fundamental frequency (60Hz in the U.S). Problems associated with harmonics include waveform distortions, voltage sags, reduced power generation efficiency, and decreased performance and durability of electrical equipment, etc. Common power electronic equipment, such as AC-DC rectifiers, DC-DC converters, and AC-AC converters, contribute to harmonic generation. Using FFT analysis of MATLAB, the output voltage of the inverter without any filter is found to contain lots of harmonic due to the switching operation of the IGBT transistors. The total harmonic distortion (THD) is 68.37% as shown on Figure 16 and Figure 17. Therefore, a low-pass LC filter is used to reduce the harmonic to create a sine wave with acceptable tolerance of THD. The filter cut-off frequency is specified at 65Hz, and inductance value of L=100mH with the corresponding C= 59.953µF is used to construct the LC low-pass filter. As shown in Figure 18 and Figure 19, the output of the filtered signal is almost ideal with a THD of 1.08%, which is well within the limits of 5% individual harmonics, or 8% of total harmonic distortion for voltage less than 1kV, as specified by IEEE 519-2022.

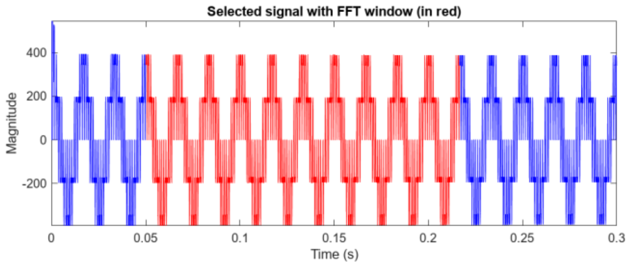


Fig. 16: Output voltage of the inverter
*Source: created by the authors.*

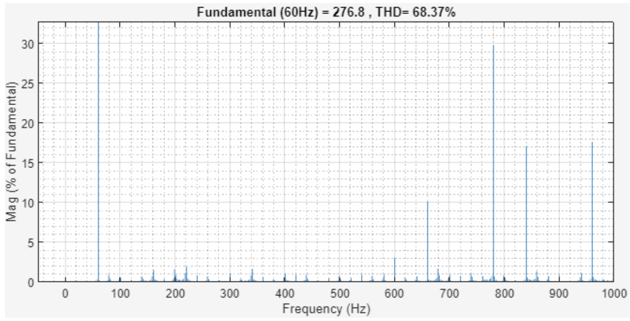


Fig. 17: FFT analysis of raw output voltage of the inverter
*Source: created by the authors.*

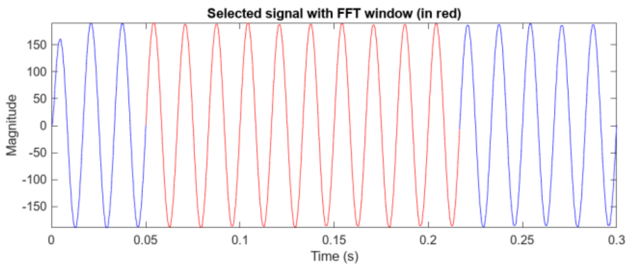


Fig. 18: Output voltage of a low-pass filter (cut-off frequency is 65 Hz).
*Source: created by the authors*

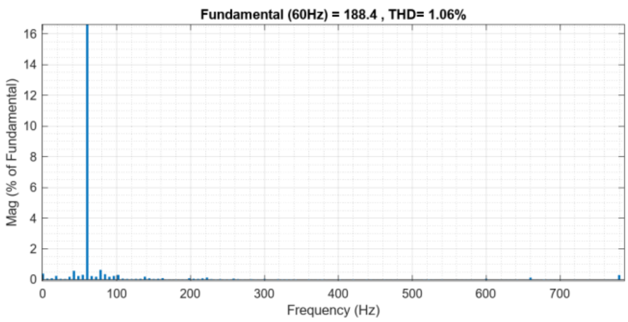


Fig. 19: FFT analysis of raw output voltage low-pass filter (cut-off frequency is 65 Hz)
*Source: created by the authors.*

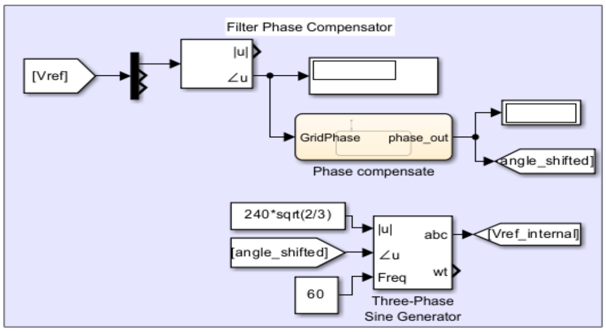

Fig. 20: Phase compensation for the low-pass filter
Source: created by the authors.

## 3.2 Filter Phase Shift and Phase Compensation

As said previously, the LC filter used in the system can eliminate the harmonics of the inverter. However, after further analysis, it is realized that the filter also introduces a certain amount of phase shift. The primary purpose of an LC filter is to filter out harmonics of the input signal by selectively allowing certain frequencies to pass through, also called cut-off frequencies. However, due to the reactive nature of inductors and capacitors, the filter can introduce phase shifts, in this case, an undesirable 85-degree, measured using Fourier block provided by MATLAB Simulink toolbox. The filter is considered very reactive, suggesting that is has a strong impact on the phase characteristics of the output signal. The substantial phase shift introduced by its reactive components, causing the output signal to misalign with the reference voltage from the grid.

There are several ways to counter the phase shift introduced by an LC filter. Adjusting inductor and capacitor values may help reduce the phase shift, however, it will also change the efficiency of the filter and THD must be maintained within the acceptable range. Some other methods are using higher order filters, digital signal processing (DSP) technique, or implementing phase compensation. This study deploys a phase compensation technique in the design to help minimize the phase difference introduced by the low-pass filter. Figure 20 shows the phase compensation implementation using MATLAB Simulink blocks.

In the investigation of grid voltage signals, the initial step involves the acquisition of voltage data from the grid, which is subsequently processed through a Fourier block to derive the phase angle in degrees for the first phase, denoted as $V_a$. The voltage $V_a$ taken from the grid is fed through a Fourier block to obtain the phase angle in degree. Since it is already known that the low-pass filter introduced an 85-degree lagging in phase in the initial analysis, we need to advance the reference signal by 85-degree to align the output signal of the filter with the grid voltage. Due to the limitation of MATLAB simulation, it is challenging to introduce phase shift instantaneously during simulation, the phase angle of the grid signal is fed through a state flow logic block of MATLAB to add 85-degree to the original grid phase to obtain the new compensated angle. This new angle was then used to generate a signal that is identical to the grid signal, with the phase angle of 85-degree advance as shown in Figure 21.

The generated signal is then used as a reference signal to feed through the phase lock loop and obtain the desired signal output after the low-pass filter. The utilization of this adjusted reference signal within the phase lock loop facilitates the extraction of the desired output signal through the low-pass filter. Using this comprehensive methodology, this study design ensures an accurate alignment of signals while also accounting for the inherent phase lag introduced by the low-pass filter.

## 3.3 Simulation Results and Analysis

The phase shift is introduced to the grid signal from time t = 0.1s to t = 0.3s. Figure 22 shows the direct $V_d$ and the quadrature $V_q$ during the operation of the system. In a phasor representation, active power (real power) aligns along the horizontal axis (the real axis), while reactive power aligns along the vertical axis (the imaginary axis). The 90-degree phase difference is characteristic of the relationship between active and reactive power components in electrical systems. This arrangement is fundamental to understanding power factor and the interplay between real and reactive power in AC circuits.

Fluctuations during this time can be observed from the active and reactive output scope right at the moment of phase shift is introduced. However, the active and reactive components remain 90-degrees apart from each other for the rest of the time.

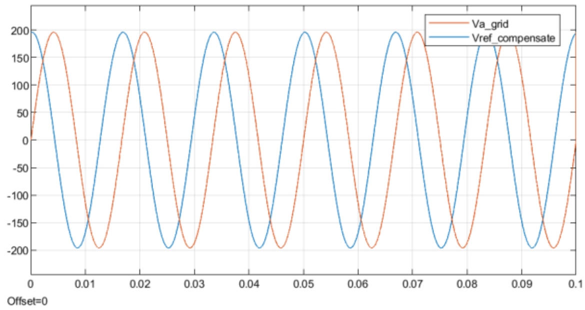

Fig. 21: Phase Va of the grid and the corresponding reference voltage advanced by 85-degree
*Source: created by the authors.*

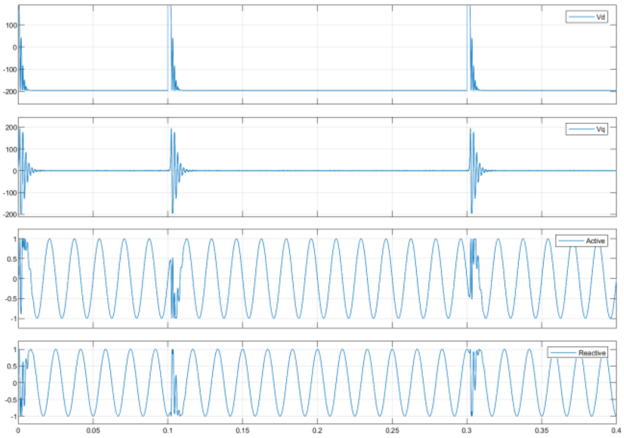


Fig. 22: $V_d$, $V_q$ and active, reactive components of the signal
*Source: created by the authors.*

Table 1. Grid phase and output of LC filter phase during phase shift of the grid

| Grid phase shift (degrees) | Grid phase (degrees) | LC filter output phase (degrees) | Phase different (degrees) |
|---|---|---|---|
| +15 | 14.46 | 13.98 | 0.48 |
| +45 | 44.46 | 44.52 | 0.06 |
| +75 | 74.46 | 74.88 | 0.42 |
| +90 | 89.46 | 89.42 | 0.04 |

*Source: created by the authors*

It is also observed that $V_q$ changes at the time of phase shifting, but then $V_q$ is driven to 0, indicating that the phase difference between the output and reference signals is minimal, hence indicates that the PLL successfully locked onto the frequency and phase of the reference signal.

Table 1 shows the phase shifts introduced to the grid using a three-phase programable voltage source from the Simulink specialized power toolbox. The phase shifts were introduced, ranging from 15 degrees to 90 degrees, for better visualization of the output synchronized with the grid voltage. Figure 23 and Figure 24 in Appendix show the output Phase A of the grid voltage and post filter output with a phase shift of 20 degrees and 90 degrees introduced at time t =0.1s. It takes approximately 0.01 seconds for the output signal to synchronize with the grid voltage.

The simulation results show that the proposed SRF-PLL based synchronization system is successful in ensuring that the inverter output is properly synchronized with the grid voltage. It meets the key requirement for V2G operation of EV (i.e., discharging the vehicle battery power into the grid). It is also worth noting that, with the integration of the internal reference signal generator within the PLL, the inverter can also operate during grid power outages (i.e., it does not need the grid voltage to function). This enables EV owners to utilize their vehicle batteries for off-grid applications, such as back-up power and other mobile power usage.

## 4 Control of EV Batteries for Supporting the Power Grid

Inductive load appliances, such as washing machines, air conditioners, fans and vacuum cleaners are quite common electrical devices in residential uses. In heavy load condition, the inductive loads can cause negative effects to the distribution grid. These effects can be even more prevalent in commercial settings due to larger and more frequent use of equipment such as motors, transformers, and other inductive components. In both cases, inductive loads increase reactive power demand, leading to reduced power factor, voltage drops and putting more stress on distribution infrastructure.

To overcome the negative effects induced by the heavy use of inductive loads, utility companies often implement power factor correction methods to mitigate the effects of inductive loading and capacitor banks is a common and effective method to maintain power factor. Figure 2 shows a shunt capacitors used in distribution grid for reactive power compensation.

However, switching interaction between capacitor banks and the grid does have some downsides. Some of the drawbacks of switching capacitor banks are inrush current, over voltage of the system, inducing stress to the circuit breaker and the shunt capacitors due to over voltage, [27].

Fig. 26: Shunt capacitors used in distribution grid for reactive power compensation
*Source: [26].*

## 4.1 BESS Simulink Integration

To examine the impact of shunt capacitor switching and the use of BESS to absorb excess reactive power, the BESS and control system, developed by [28] was adopted and modified to run the simulation under different scenarios. Figure 25 (Appendix) shows the implementation of a power distribution system with BESS, solar PV farms and shunt capacitors installed near the load location.

The shunt capacitors used in the system were intentionally oversized to create an overvoltage condition after switching on. Additionally, the state flow logic adopted from the original BESS system in [28] for controlling the power converter in each battery bank was modified to react faster, increasing the speed to improve the system's reaction time. The control system was also adjusted to measure the change in Phase A voltage and allow the BESS to absorb reactive power for quick stabilization of the voltage at the load location.

## 4.2 BESS with Shunt Capacitor Switching in Grid Operation

BESS can be very effective in managing overvoltage issues associated with shunt capacitor switching, [28]. The storage system can provide a dynamic and flexible approach to grid management and provide rapid response to voltage fluctuations since BESS can react very quickly by using fast power electronics, [28]. It can also act as a motor and a generator by controlling the switching operation of electronics switching elements, [28].

In the study [28], a shunt capacitor is switched on to compensate for the weak power line created by a high inductive load. The initial setup of the load is a 5 MW load with 1 MVAR of inductive power, representing a high inductive load during peak hours. A voltage prop is placed on Phase A of the power distribution line near the load location to measure the voltage. In Figure 27, the phase voltage was measured at 0.952 per unit.

The low voltage (0.952 per unit) indicates that the system is not working at its optimal performance. It is usually accompanied by a low power factor. This is typically caused by the presence of inductive load appliances like electric motors and transformers. Both residential and commercial consume reactive power for operation, thus increasing the overall demand for current. The increased current demand has a significant role in amplifying the voltage drops in the distribution system, particularly prevalence near the load location.

Such voltage drops not only negatively impact the efficiency of the electrical power system but also affect the stability and reliability of the electrical equipment of consumers. This problem creates significant challenges for industrial consumers, especially those in manufacturing. These customers rely heavily on consistent and sTABLE voltage supply to operate efficiently and economically. Notably, they also employ extremely sensitive equipment, such as CNC machines, large motors, and assembly lines. Voltage drops might seize the operation of these motors, or even worse, halt the entire operation of the manufacturing line. Unexpected downtime in manufacturing is particularly critical. Interruptions of production line causes delayed order fulfillment. Consequently, heavy financial losses may happen.

To bring voltage back to the optimal level for the load, a 1.4-MVA shunt capacitor is switched on at time t = 0.25s, where the phase voltage oscillates near the maximum value to exaggerate the effect of capacitor switching.

While shunt capacitors can improve power factor and support voltage levels, they can create overvoltage under some circumstances, such as excessive reactive power, where it provides more reactive power than needed to counteract the inductive load. This can cause the voltage levels to rise above the normal operating voltage of the system. Incorrect sizing and configuration of shunt capacitors also leads to voltage issues. Over-sizing capacitors can also lead to localized overvoltage conditions, especially in networks with dynamic load characteristics.

To mimic overvoltage problem, the size of the 1.4-MVA shunt capacitor is intentionally configured to provide overvoltage after switching on. Figure 29 shows the voltage measured on Phase A near the load location, after switching on the shunt capacitor at time t = 0.25s. In order to mitigate the problem, sophisticated and complex monitoring must be deployed to monitor and regulate the system in real time. In this study, the proposed idea is to use the BESS, which are the battery packs of the EVs connected to the grid, to absorb the excess reactive power generated from connecting shunt capacitors, thus protecting the system from overvoltage.

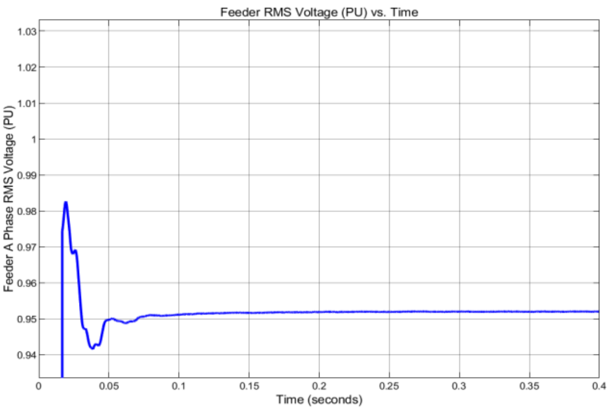


Fig. 27: Low voltage measured at Phase A near the load location, due to high inductive load and weak power distribution line
*Source: created by the authors.*

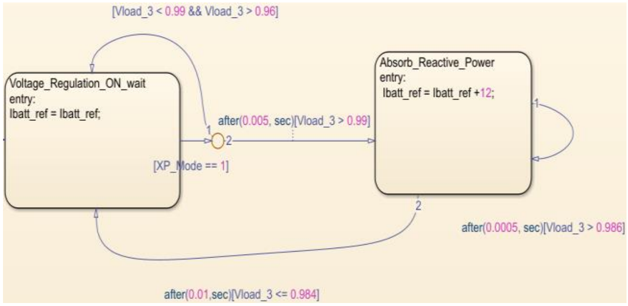


Fig. 28: Modified operation logic of BESS to absorb reactive power measured near load site
*Source: created by the authors.*

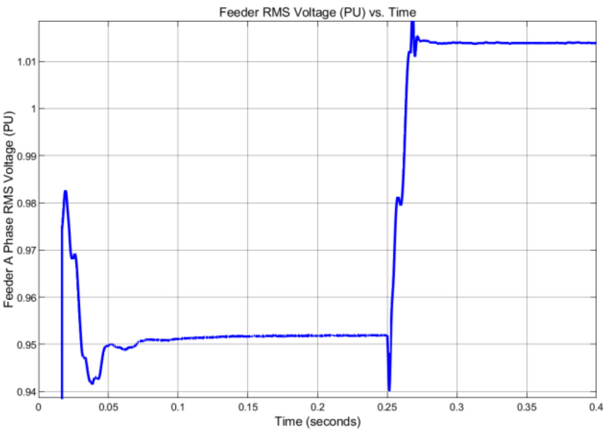


Fig. 29: Overvoltage after shunt capacitors switched on at t = 0.25s
*Source: created by the authors.*

The BESS system used in Bonilla-Le model is rated at 2.8 MW and a Tesla Model S battery pack is rated at 100 kWh, which means the BESS is equivalent to 28 Model S cars connected to the grid. Figure 30 shows a partial configuration of the BESS. It consists of four 700-kW battery banks (total 2.8 MW), connected to the grid via a 440V/12kV step up transformer. Figure 31 shows the BESS real, reactive and apparent power.

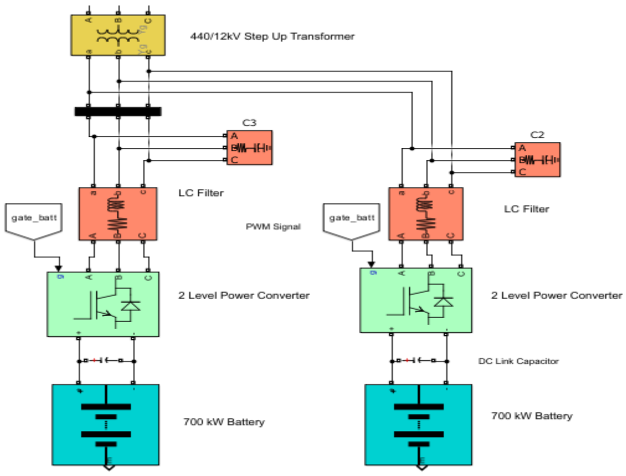


Fig. 30: BESS design (partial)
*Source: [28].*

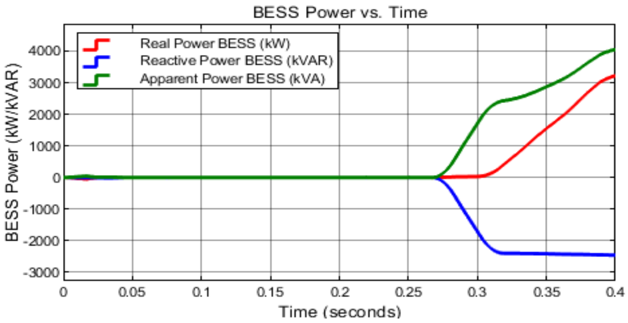


Fig. 31: BESS real, reactive and apparent power
*Source: [28].*

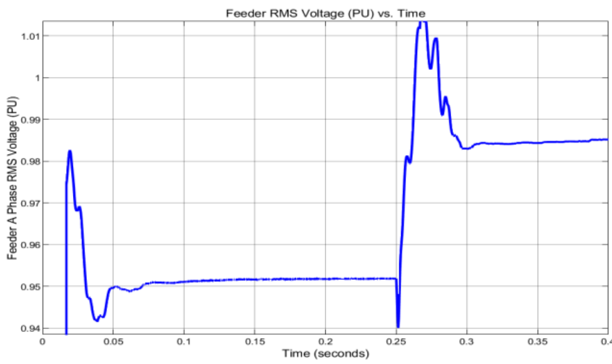


Fig. 32: BESS regulated per-unit voltage measured at Phase A load line
*Source: created by the authors.*

To control the operation of the power converter used in each battery bank, a state flow logic is used to generate the control signal by using a PWM block from Simulink. Figure 28 shows the modified state flow logic of the control unit. Phase A per unit voltage near the load location is measured and stored as Vload3 variable and fed into the state flow to regulate the voltage. The variable Ibatt_ref is used to control the operation of the IGBT switches to convert the DC power of the battery to AC. In Figure 19, Ibatt_ref is added +12 after 0.005 seconds, indicates that the IGBTs operate to make the battery absorb reactive power. A negative sign indicates that the battery is providing reactive power to the system.

As shown on Figure 29, at the moment the shunt capacitor is connected (t=0.25s), the per-unit voltage of Phase A briefly drops, then quickly recovers, and remains above 1.0 per unit. In Figure 31, it is observed that 2.38 MVAR of reactive power, measured at the BESS, is absorbed in 45ms after the shunt capacitors are switched on to bring down the per unit voltage at the load location. The state flow logic is modified to measure the change in Phase A voltage and allow the BESS to react accordingly. In this case, reactive power is absorbed by the BESS (i.e., battery packs of EVs plugged into the grid) to bring the voltage down to the appropriate level.

As mentioned, the BESS is controlled by power electronics components, thus the response speed can be increased, [28]. Hence, the modified control logic response time is increased 10 times to provide quicker reaction time of the system and successfully regulate the voltage after shunt capacitor is switched on.

Figure 32 shows the regulated per unit voltage of Phase A at the load. It takes approximately 32.468ms to bring down the load voltage from over 1.01 per unit to 0.985 per unit. The total time for the load voltage to stabilize after the shunt capacitor is switched on is approximately 60ms.

The simulation results show that the battery packs of grid-connected EVs can be used successfully to mitigate overvoltage situations due to shunt capacitor switching on the grid. This suggests another usage of V2G technology for supporting the grid while bringing economic benefits to the EV owners.

# 5 Conclusion

The first part of this study focuses on implementing a synchronous rotating frame phase lock loop (SRF-PLL) for synchronizing EV bidirectional charger output with the grid in V2G operation. This study also explores a technique to deal with phase differences between the grid and the bidirectional charger, which occur due to the grid daily fluctuations, in a V2G context. The last part considers operating the battery packs of grid connected EVs as a BESS to manage grid voltage during shunt capacitor switching situations.

The outcomes of this research have led to the following conclusions:

1) The proposed SRF-PLL system is successful in ensuring alignment of EV bidirectional charger voltage output with the grid. This satisfies a core requirement for EV chargers to interface with the power system in V2G operation.
2) The ability of the bidirectional charger to align with the changing phases of the grid quickly is demonstrated via simulation. This shows that the proposed phase compensation method is effective.
3) Integration of the internal 60-Hz power source for the PLL allows the bidirectional charger (in discharging or inverter mode) to function during grid power outages. This can bring lots of benefits to EV owners because they can utilize their vehicle batteries for multiple off-grid home and mobile power supply applications.
4) It has been proven that EV batteries packs can be effectively used as BESS in power transmission setting to absorb excess reactive power and stabilize voltage in shunt capacitor switching situations.

By addressing some challenges for V2G technology, this study contributes to accelerating adoption of the technology for supporting the power grid while bringing economic benefits for the EV owners. The outcomes help extend EV capability, broadening their practical use for both the vehicle owners and power grid operators. This, in turn, facilitates wide penetration of EVs for transforming the transportation sector, lowering harmful emissions, and protecting the environment.

*Acknowledgement:*
The student author Nhat Nguyen would like to express his deepest gratitude to the Master project committee members, Prof. Gerald Herder, and Prof. Zekeriya Aliyazicioglu for their invaluable time and feedback. A special word of thanks to his advisor and chair member of the thesis committee, Dr. Ha Thu Le, whose expertise, understanding, and patience have been crucial to the completion of this research.

*References:*

[1] S. Media, "Save Money on Transportation | Clean Vehicle Rebate Project", [Online]. https://cleanvehiclerebate.org/en/ev/benefits/save-money (Accessed Date: January 10, 2026).

[2] M. Jayachandran, C. R. Reddy, S. Padmanaban, and A. H. Milyani, "Operational planning steps in smart electric power delivery system," *Scientific Reports*, vol. 11, no. 1, p. 17250, 2021/08/26 2021, doi: 10.1038/s41598-021-96769-8.

[3] G. Hering. "EV Impact: Rise of electric vehicles heightens grid-integration imperative " S&P Global Market Intelligence, [Online]. https://www.spglobal.com/marketintelligence/en/news-insights/latest-news-headlines/ev-impact-rise-of-electric-vehicles-heightens-grid-integration-imperative-66620630 (Accessed Date: January 10, 2026).

[4] J. Glueck and Ha Thu Le, "Impacts of Plug-in Electric Vehicles on local distribution feeders," presented at the IEEE Power & Energy Society General Meeting, 2015.

[5] N. Groom and T. Bellon. "EV rollout will require huge investments in strained U.S. power grids." Reuters, [Online]. https://www.reuters.com/article/us-usa-weather-grids-autos-insight/ev-rollout-will-require-huge-investments-in-strained-u-s-power-grids-idUSKBN2AX18Y (Accessed Date: January 10, 2026).

[6] "Influx of Electric Vehicles Accelerates Need for Grid Planning." Pacific Northwest National Laboratory (PNNL) , [Online]. https://www.pnnl.gov/news-media/influx-electric-vehicles-accelerates-need-grid-planning (accessed 1 June 2023.

[7] C. B. Jones, M. Lave, W. Vining, and B. M. Garcia, "Uncontrolled Electric Vehicle Charging Impacts on Distribution Electric Power Systems with Primarily Residential, Commercial or Industrial Loads," *Energies*, vol. 14, no. 6, 2021, https://doi.org/10.3390/en14061688.

[8] "Impact of Electric Vehicles on the North American Power Grid." Enverus, [Online]. https://www.enverus.com/blog/impact-of-electric-vehicles-on-the-north-american-power-grid/ (Accessed Date: January 10, 2026)..

[9] J. Hsu. "Too many electric cars charging at night may overload electrical grid." NewScientist, [Online]. https://www.newscientist.com/article/2339237-too-many-electric-cars-charging-at-night-may-overload-electrical-grid/ (Accessed Date: January 10, 2026).

[10] "Electric Vehicle (EV) Impact Report," Power Technology Research, 2022, [Online]. https://powertechresearch.com/ev-impact/ (Accessed Date: January 10, 2026).

[11] "Tesla Model S Performance." Electric Vehicle Database, [Online]. https://ev-database.org/uk/car/1207/Tesla-Model-S-Performance (Accessed Date: January 10, 2026).

[12] Chris Chu, "Supporting Bidirectional Operation of Electric Vehicle-to-Grid, Vehicle-to-Home and Vehicle-to-Load (Master Thesis)," MSEE, California State Polytechnic University Pomona, Pomona, California, 2023.

[13] G. Lumley, "Power Surges: How to Protect Your Home," (in en), *BKV Energy*, 2024/03/28/T10:47:26-06:00 2024, [Online]. https://bkvenergy.com/blog/how-to-protect-home-from-power-surge/ (Accessed Date: January 10, 2026).

[14] A. Marshall. (2023) Tesla's Supercharger Strategy Starts a Winning Streak. *Wired*, [Online]. https://www.wired.com/story/teslas-supercharger-strategy/ (Accessed Date: January 10, 2026).

[15] "Time-Of-Use Residential Rate Plans." Southern California Edison (SCE) , [Online]. https://www.sce.com/residential/rates/Time-Of-Use-Residential-Rate-Plans (Accessed Date: January 15, 2026).

[16] Y. Jang *et al.*, "Grid-Connected Inverter for a PV-Powered Electric Vehicle Charging Station to Enhance the Stability of a Microgrid," *Sustainability*, vol. 13, no. 24, p. 14022, 2021, [Online]. https://www.mdpi.com/2071-1050/13/24/14022 (Accessed Date: January 10, 2026).

[17] D. o. Energy, "Building the Business Case for Bidirectional Electric Vehicles," (in en), *Energy.gov*, [Online]. https://www.energy.gov/technologytransitions/articles/building-business-case-

bidirectional-electric-vehicles (Accessed Date: January 22, 2026).

[18] H. Al Attar, M. A. Hamida, M. Ghanes, and M. Taleb, "LLC DC-DC Converter Performances Improvement for Bidirectional Electric Vehicle Charger Application," *World Electric Vehicle Journal*, vol. 13, no. 1, p. 2, 2022, [Online]. https://www.mdpi.com/2032-6653/13/1/2 (Accessed Date: January 10, 2026).

[19] "Bidirectional Charging: How to Use Your EV as a Home Battery," (in en), *CNET*, [Online]. https://www.cnet.com/roadshow/news/bidirectional-charging-and-evs-how-does-it-work-and-which-cars-have-it/ (Accessed Date: January 10, 2026).

[20] J. Ögren, "PLL design for inverter grid connection : Simulations for ideal and non-ideal grid conditions," Independent thesis Basic level (degree of Bachelor) Student thesis, TVE, 11 008, 2010, [Online]. http://urn.kb.se/resolve?urn=urn:nbn:se:uu:diva-156145 (Accessed Date: January 10, 2026).

[21] Ford. "Ford Charge Station Pro", [Online]. https://chargers.ford.com/ford-charge-station-pro (Accessed Date: January 10, 2026).

[22] F. Energy, "Fermata Energy's Newest V2X Bidirectional Charger — the FE-20 — Available Q1 2023," (in en) , [Online]. https://fermataenergy.com/article/fermata-energys-newest-v2x-bidirectional-charger- (Accessed Date: January 10, 2026).

[23] Y. Xuan, x. Yang, W. Chen, T. Liu, and X. Hao, "A Three-Level Dual-Active-Bridge Converter With Blocking Capacitors for Bidirectional Electric Vehicle Charger," *IEEE Access*, vol. PP, pp. 1-1, 12/02 2019, doi: 10.1109/ACCESS.2019.2957022.

[24] J. Xu, H. Qian, Y. Hu, S. Bian, and S. Xie, "Overview of SOGI-Based Single-Phase Phase-Locked Loops for Grid Synchronization Under Complex Grid Conditions," *IEEE Access*, vol. 9, pp. 39275-39291, 2021, doi: 10.1109/ACCESS.2021.3063774.

[25] Q.-C. Zhong and T. Hornik, *Control of power inverters in renewable energy and smart grid integration*, 1st edition ed. Chichester, West Sussex: Wiley, 2013, p. 1 online resource (439 p.).

[26] E.-E. E. Portal. "Experience in installation of new reactive power compensation on power grid: EEP", [Online]. https://electrical-engineering-portal.com/download-center/books-and-guides/electricity-generation-t-d/new-reactive-power (Accessed Date: January 30, 2026).

[27] M. Taherzadeh, R. Rostaminia, M. Joorabian, and M. Saniei, "Mitigation of capacitor bank switching transients by using SVCs in large plants instead of capacitor bank and circuit breaker," in *4th Annual International Power Electronics, Drive Systems and Technologies Conference*, 13-14 Feb. 2013 2013, pp. 321-327, doi: 10.1109/PEDSTC.2013.6506726.

[28] O. Bonilla and H. T. Le, "Multi-functional energy storage system for supporting solar PV plants and host power distribution system," *Journal of Energy Storage*, vol. 73, p. 108933, 2023/12/01/ 2023, https://doi.org/10.1016/j.est.2023.108933.

**Contribution of Individual Authors to the Creation of a Scientific Article (Ghostwriting Policy)**

The authors equally contributed in the present research, at all stages from the formulation of the problem to the final findings and solution.

**Sources of Funding for Research Presented in a Scientific Article or Scientific Article Itself**

No funding was received for conducting this study.

**Conflict of Interest**

The authors have no conflicts of interest to declare that are relevant to the content of this article.

# APPENDIX

*Boost converter calculations for discharging operation:*
Switching frequency f = 25000 Hz
Given input voltage VIN = 450 V
Desired output voltage VOUT = 460 V
Given maximum load current ILOAD_MAX = 80 A
Desired ripple voltage Vripple = 0.005 %
Rload = $\frac{V_{out}}{I_{load\_max}}$ = 5.7500 Ω
D = $1-\left(\frac{V_{in}}{V_{out}}\right)$ = 0.0217

Minimum inductance Lmin = $D*(1-D)^2*\frac{R_{load}}{2f}$ = 2.3925 μH

Capacitance C = $\frac{D}{R_{load}*V_{ripple}*f}$ = 30.246 μF

*Filter design calculations:*
$$f_c = \frac{1}{2\pi\sqrt{LC}}$$
$$L = \frac{1}{4\pi^2(f_c)^2C}$$
$$C = \frac{1}{4\pi^2(f_c)^2L}$$
Low-pass filter cut-off frequency is 65Hz
Fc = 65Hz; L = 100mH;
$C = \frac{1}{4\pi^2(65Hz)^2(100\text{mH})}$ = 59.953 μF

*Phase compensation calculation:*
Carier frequency fc = 17.7135 Hz
Filter inductance value L = 272.515 mH
Filter capacitance value C = 22 μF; R = 33 Ω;
Inductive reactance Xl = $2\pi*f_c*L$ = 30.3302 Ω

Capacitive reactance Xc = $\frac{1}{2\pi f_c C}$ = 408.4069 Ω

Calculated phase shift = $\tan^{-1}(\frac{X_l-X_c}{R})$ = -1.4837 rad

Phase shift (degree) =$phaseshift*\frac{180}{\pi}$ = -85.0116 deg.

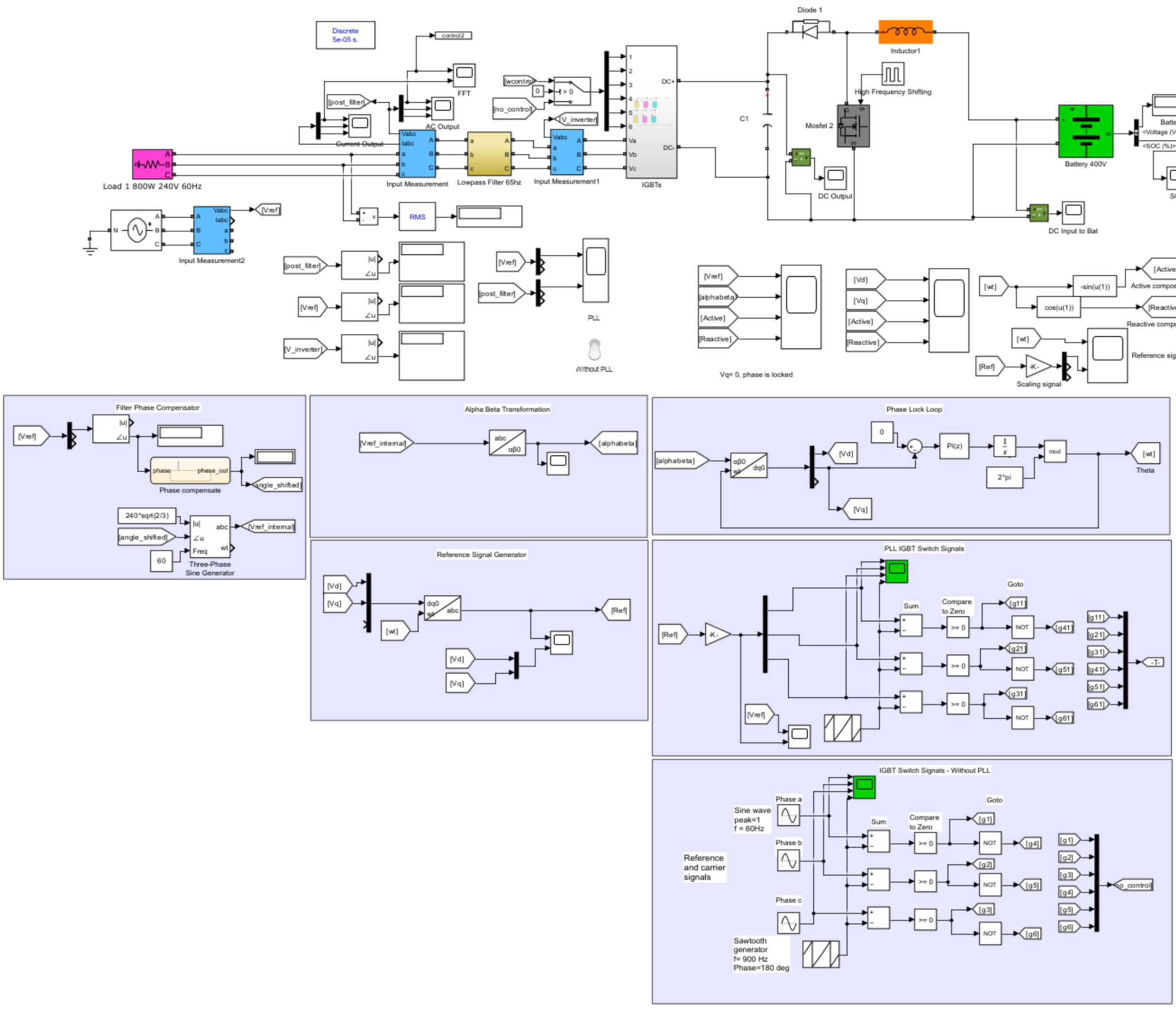


Fig. 11: MATLAB Simulink implementation of EV discharging system for V2G application. The grid is represented using a 3-phase 240-V RMS 60-Hz variable AC source to introduce phase shifts during simulation. The output of the IGBT-based inverter is connected to a lowpass filter and the inverter output signal is measured after the filter

*Source: Created by authors*

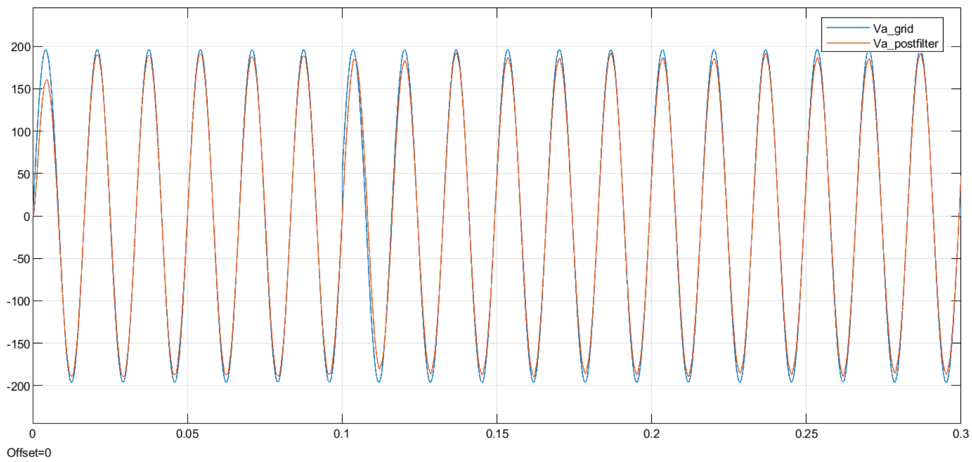


Fig. 23: Scope image of Phase A voltage, obtained from the grid signal, compared to the corresponding output signal obtained after the LC filter; Phase shift 20-degrees introduced at time t = 0.1s

*Source: Created by authors.*

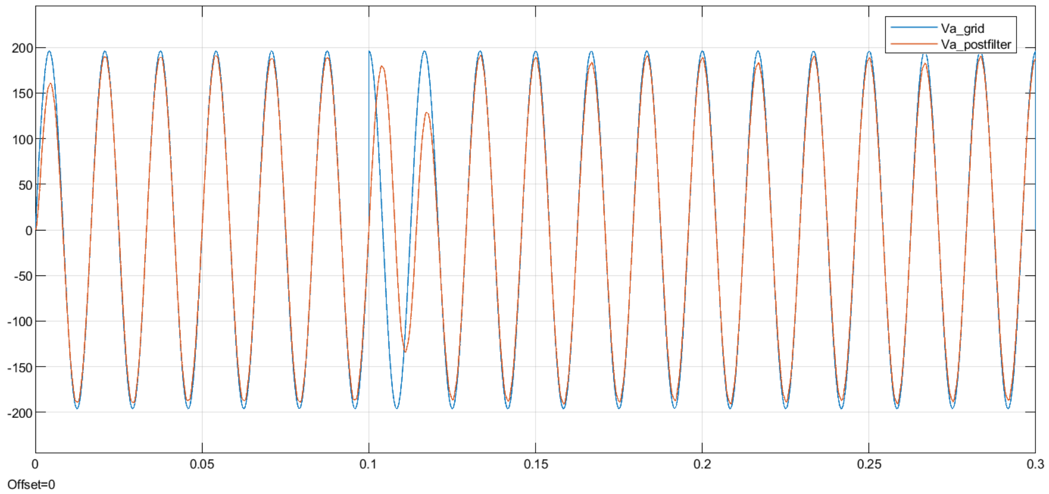


Fig. 24: Scope image of Phase A voltage, obtained from the grid signal, compared to the corresponding output signal obtained after the LC filter; Phase shift of 90-degrees introduced at time t = 0.1s

*Source: Created by authors.*

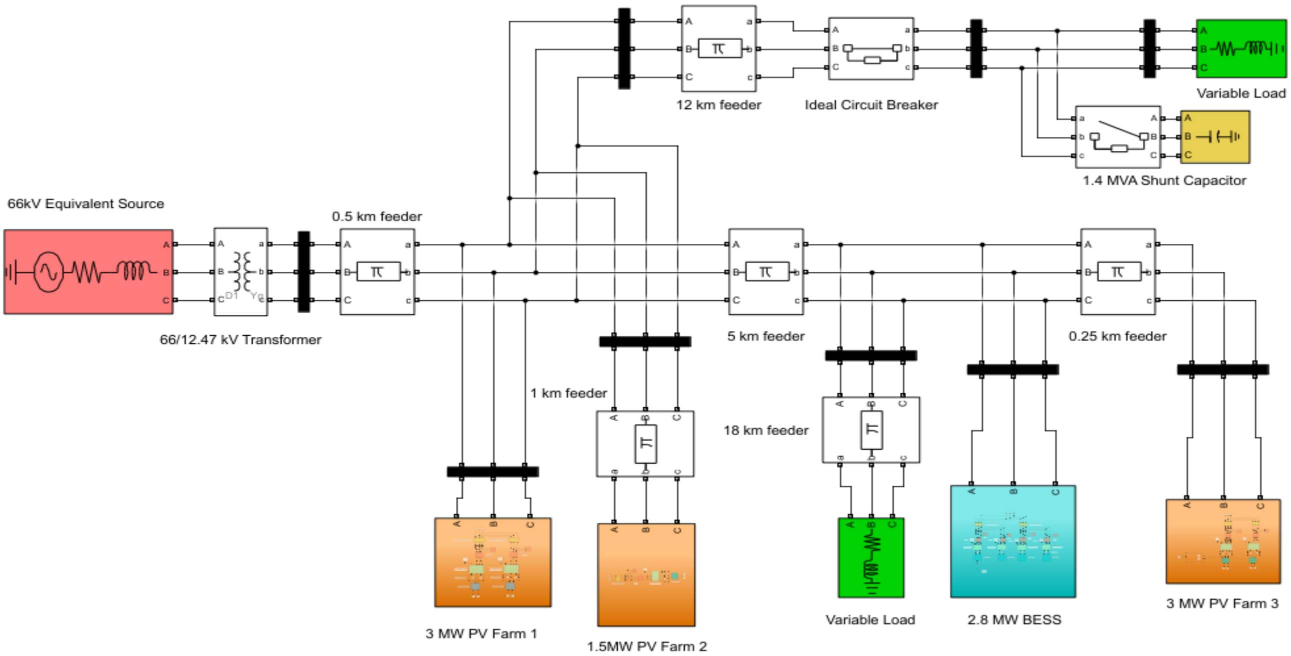


Fig. 25: MATLAB Simulink implementation of power distribution system with BESS, solar PV farms and shunt capacitors installed near load location, adopted from a prior study

*Source: [28]*